Chapter 1

Introduction:

Magnetic Interactions in MRI and Molecular Materials

Introduction

The phenomenon known as magnetism has caused wonder ever since the discovery of lodestone by the Chinese in the fourth century. While magnetism resulting from charge flow was described by Maxwell in the mid 1800's, the explanation of intrinsically magnetic materials such as lodestone (known now as magnetite) requires the physics of quantum mechanics. It is now well accepted that the physical attribute of subatomic particles called 'spin' is essential for the manifestation of magnetism in intrinsically magnetic materials. Although the particles themselves do not spin, the term suggests parallels with the classical idea of angular momentum resulting from the movement of an entity about its center of mass. Electrons, protons and neutrons all have intrinsic spin that gives rise to a magnetic dipole moment. The magnitude of this moment depends inversely on the mass of the particle; hence electrons have a moment that is ~1836 times larger than protons. Thus, the major contribution to the magnetism in magnetite is due to the electrons. The intrinsic spin angular momentum in electrons, protons and neutrons is quantized and labeled with a quantum number. All three types of particles have a spin quantum number equal to 1/2. The movement of the negatively charged electron about the positive nucleus in an atom also gives rise to a magnetic dipole moment. This is referred to as the orbital angular momentum, and it too is quantized.

The various angular momenta described above are vectors and can interact with each other and with external magnetic fields. In atomic physics the spin quantum number, *S*, describes the sum of the electron spin quanta, the orbital quantum number, *L*, describes the sum of the electron orbital angular momentum quanta and the nuclear spin

quantum number, *I*, describes the sum of the nucleon spin quanta. The interactions of *S*, *L* and *I* both intra- and inter-atomically and with external magnetic fields provide the foundation for the phenomena investigated in this dissertation.

Zeeman Effect

Application of an external magnetic field to a non-zero quantum angular momentum state results in the removal of the energetic degeneracy of the levels within that state. The degeneracy of a state is given by $2X + 1$ ($X = S, L, I$) levels. For the simple system where the quantum number is 1/2 (such as the hydrogen nucleus in a water molecule consisting of one proton with $I = 1/2$) this gives rise to two levels, one aligned with the magnetic field and one opposing the field (Figure 1-1 top). The energy difference between the levels is directly proportional to the strength of the magnetic field H_o:

$$\Delta E = g\left(\frac{eh}{4\pi mc}\right)H_o \qquad (1)$$

where *g* is the *g*-factor for the particle under study (electrons, protons or neutrons) and *m* is the mass of the particle.

When an ensemble of spins is exposed to a magnetic field, the resulting levels, having different energies, are populated based on a Boltzmann distribution. This difference in population results in a bulk magnetization vector, $\boldsymbol{M}$, which, due to the arbitrary phase of the individual magnetic moments, $\boldsymbol{\mu}$, aligns with the magnetic field, $\boldsymbol{H_o}$ (Figure 1-1 bottom). It is the quantity $\boldsymbol{M}$ that provides the basis for modern FT-NMR, EPR and MRI.

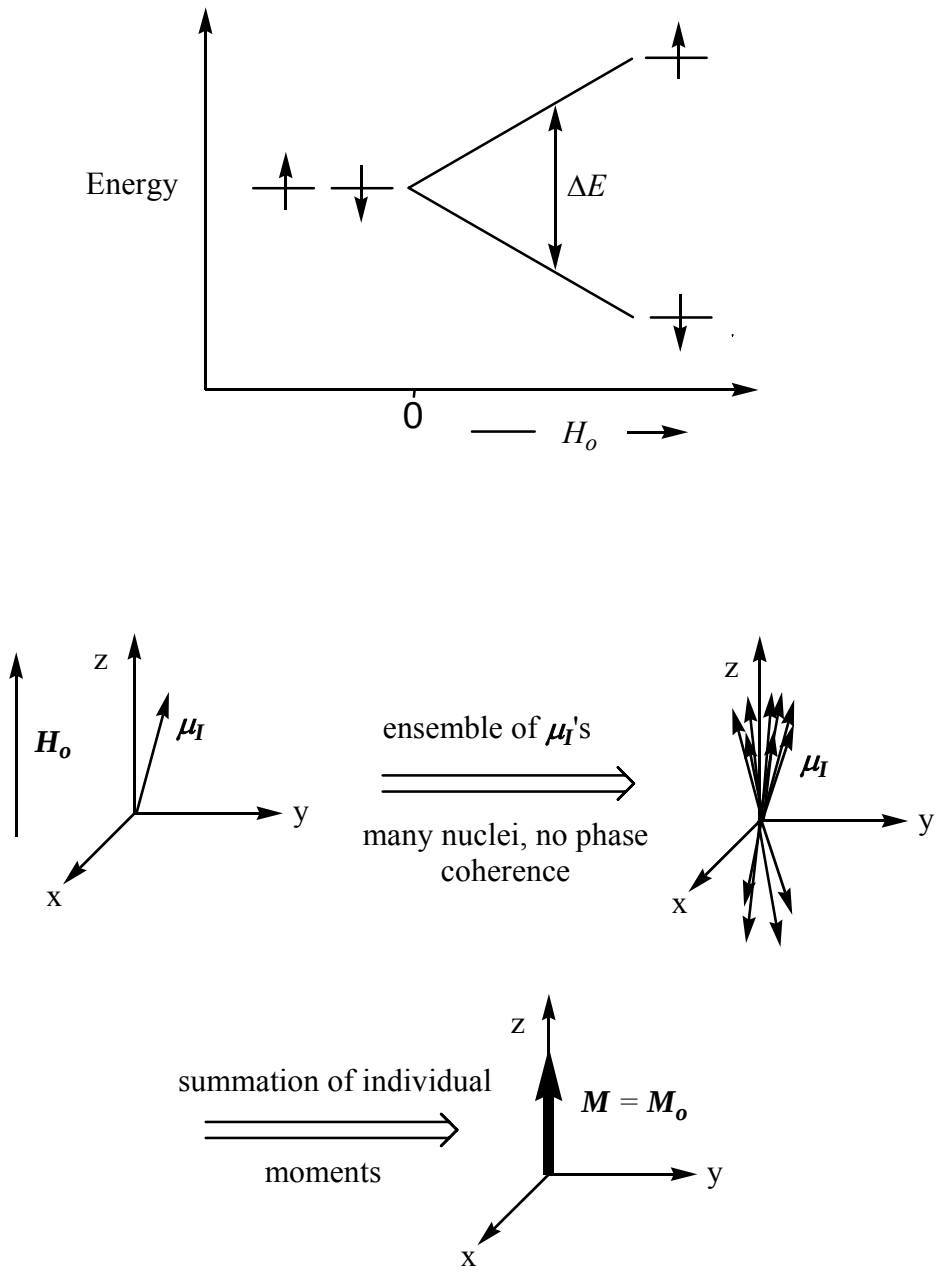

Figure 1-1: The Zeeman effect on a spin 1/2 particle as a function of applied magnetic field strength, H_o (top). The bulk magnetization, $\boldsymbol{M}$, results from an ensemble of magnetic moments in an applied magnetic field (bottom).

Irradiation of the simple spin 1/2 system in a magnetic field with a photon of energy equal to the energy splitting between the two levels results in transfer of the system from the lower energy level to the upper level. Since the energy splitting depends inversely on the mass of the particles under consideration (Equation 1), the splitting between levels will be much greater for electrons compared to nuclei at a given H_o. Since the Zeeman splitting in general is smaller than k_BT at room temperature (separations being in the RF (radio frequency) range for nuclei and in the microwave range for electrons using commercially available superconducting magnets), the population difference between the two levels is quite small. This presents a fundamental sensitivity problem for nuclei-based techniques such as NMR and MRI.

Types of Magnetism

The types of magnetic behavior that arise in molecules and materials resulting from intra- and inter-atomic interactions can be classified into two broad categories, systems that display long-range interaction and systems that do not. While molecular crystals typically do not demonstrate long-range magnetic order, an understanding of the behavior of electrons and nucleons in these systems provides a foundation for comprehending the long-range interactions that generate bulk magnetism.

The magnetic response of a system is characterized by its magnetization vector, $\boldsymbol{M}$, as a function of applied field, $\boldsymbol{H_o}$ and temperature, T. Chemists prefer to use the magnetic susceptibility, χ, which is the ratio of $\boldsymbol{M/H_o}$. This quantity is independent of $\boldsymbol{H_o}$ only if the magnetization is a linear function of applied field, which it typically is not for materials displaying long-range ordering. The molar magnetic susceptibility, χ_m, is

the magnetic susceptibility per mole of substance.

Diamagnetism

Electrons are fermions due to their half-integer spin and are therefore governed by the Pauli exclusion principle. This means that only one electron can occupy a given level defined by spatial and spin quantum numbers. Since spatial states in molecules are typically spaced far apart in energy it is favorable for the electrons in most molecules to doubly occupy a spatial state. To do this and still fulfill the exclusion principle, the electrons must have differing spin. Thus most molecules, particularly organic molecules, contain equal numbers of electrons in each of the two levels allowed by the spin 1/2 quantum number. The result is zero net magnetization arising from the sum of the intrinsic spin magnetic moments of the electrons in the molecule. However, the molecule will still respond to an external magnetic field due to the magnetism that arises from the *motion* of the negatively charged electrons. This magnetism is known as diamagnetism and is a characteristic of all molecules and materials composed of atoms. The diamagnetic response of a system opposes the applied field and hence displays a negative susceptibility that is independent of temperature.

Paramagnetism

The presence of unpaired electrons in an atom or molecule generates a net magnetization resulting from the sum of the spin angular momenta of the electrons. The magnitude of this spin-only magnetization is determined by physical constants and the spin quantum number, *S*, which has a value of the number of unpaired electrons

multiplied by the electron spin of 1/2. When an external magnetic field is applied to a paramagnetic system the net magnetization aligns with the field. Thus paramagnetism opposes diamagnetism. The two types of magnetism are similar however because the magnetic moments in a para- or diamagnetic ensemble only order when they are exposed to an external magnetic field. Removal of the field results in each magnetic moment of the ensemble having an arbitrary direction and thus the net magnetization of the bulk system is zero. Paramagnetic systems typically have paired electrons and thus contain a diamagnetic contribution that must be accounted for before the paramagnetic behavior can be analyzed. For comparison, the paramagnetic response is usually two to three orders of magnitude larger than the diamagnetic response.

Paramagnetic systems, such as compound **2** in Chapter 4 or the gadolinium(III) ion used for MRI contrast agents, display magnetic susceptibilities that depend on temperature. For idealized Curie paramagnetic behavior the susceptibility, χ, depends inversely on temperature; thus a plot of χT versus T will be linear with a slope of zero. Deviations from linearity indicate the presence of more complex magnetic behavior that may result from long-range magnetic interactions, magnetic exchange coupling or contributions from the orbital angular momentum of the electrons. The Van Vleck formalism takes into account higher-lying electronic states in the system that can generate temperature independent paramagnetism (TIP). For a system comprised of one electronic state the Van Vleck description reduces to the Curie representation. The magnetic superexchange interaction discussed later in this chapter and in Chapters 3 and 4 gives rise to a more complicated paramagnetic system comprised of two or more paramagnetic ions. This interaction can also result in longer range magnetism and magnetic order as

discussed below and in Chapter 4.

Nuclear paramagnetism

While the magnetism resulting from nuclei is dwarfed by the lighter electrons, nuclei with non-zero I values may interact with each other giving rise to the chemical shifts and coupling constants seen in high-resolution NMR spectra. Perhaps the most well studied nucleus is the proton of the hydrogen atom. As mentioned above, the hydrogen atom nucleus is a two-state system with $I = 1/2$. The water molecule contains two hydrogen atoms, and it is the nuclear spins from these atoms that are manipulated to generate an MR image. In the presence of an external magnetic field an ensemble of water molecules gives rise to a net magnetization, $\boldsymbol{M}$, resulting from the thermal population of the spin states of the hydrogen nuclei that are split by the Zeeman effect. In the absence of a field, the nuclear spins do not show any long-range correlation; hence the magnetism of water behaves in a fashion analogous to the paramagnetism described above for electrons.

Ferro-, antiferro- and ferrimagnetism

When the magnetic moments from unpaired electrons that give rise to paramagnetism interact, the system can display long-range magnetism. These types of interactions are responsible for the type of magnetism apparent in a bar magnet and in the lodestone example discussed above. Typically the long-range order is observed in crystalline solids where the paramagnetic centers are arranged in a periodic lattice. Here, adjacent paramagnetic centers interact and the magnetic moments can align with respect

to each other. If the moments align parallel to each other the system is said to be ferromagnetically coupled and the resulting magnetic behavior is described as ferromagnetic. Conversely, if the moments align anti-parallel to their neighbors the system is antiferromagnetically coupled. If the antiferromagnetically coupled system consists of identical paramagnetic centers then the net magnetization will be nearly zero due to a cancellation of moments caused by the anti-parallel arrangement. Systems that display this behavior are called antiferromagnets. If the system is comprised of differing paramagnetic centers that are antiferromagnetically coupled then the cancellation of moments may be incomplete, resulting in a bulk magnetization. This type of system is referred to as a ferrimagnet.

The long-range magnetism in the systems discussed in this section is intrinsic to the material and therefore the moments remain aligned in the absence of a magnetic field. Application of an external magnetic field to these systems will result in reorientation of the magnetic moments in the material. Since the moments within the material are fixed in direction due to their long-range interactions, the system can respond to the field by physically moving in space. This will occur if there is a net magnetization to the material.

Although the material may display long-range magnetic interactions, the system may not always exhibit a macroscopic moment. This is due to the arrangement of ensembles of long-range interactions into magnetic domains. Within the domain the moments are all aligned; however the domains need not be aligned with each other. Thus, since the net magnetization from each domain adds vectorally, the result can be a small bulk magnetization. Application of a strong external magnetic field can cause the

domains to align by forcing the moments in the material to respond to the external field. The ease with which the domains align can be quantitated by the hysteresis the material displays. A soft ferromagnet is one in which the domain walls separating each domain align easily, while a hard ferromagnet requires a stronger field for alignment.

A given system will only display the irreversible behavior associated with long-range magnetic interactions if it is below a critical temperature. Above this temperature the individual paramagnetic moments do not interact on a long-range scale and the system displays paramagnetic behavior. The temperature at which this occurs for ferromagnets is called the Curie temperature, while for antiferromagnets and ferrimagnets it is known as the Néel temperature. The Curie temperature in steel is quite high and can be seen when a piece of steel is heated until it is orange-red hot. At this point it is no longer attracted to a magnet.

Superparamagnetism

Superparamagnetism refers to a type of magnetism intermediate between paramagnetism and ferromagnetism. Like ferromagnetism, the electron spins on the atoms within a superparamagnetic material are all aligned with each other. However, like a paramagnetic system, the material does not display an intrinsic magnetization in the absence of an applied field. Superparamagnetic systems are typically small in size, on the order of tens of nanometers, and consist of one magnetic domain. If the domains within a non-conducting ferromagnetic system were spatially removed from each other, each domain would behave as a superparamagnet. While superparamagnetic materials do not display intrinsic magnetization, the relaxation of the magnetization in a

superparamagnet is thermally activated and can be slow below the material's blocking temperature. When this occurs, the unrelaxed magnetization causes the material to show behavior that is analogous to ferromagnets. Low dimensional molecular compounds can display superparamagnetism (Chapter 4) and superparamagnetic iron oxide nanocrystals are important in MRI.

Magnetic Interactions

Thus far this chapter has discussed the manifestations of magnetic interactions but has mentioned little regarding the interactions themselves. This section discusses the magnetic interactions that occur through space to form the basis for the gadolinium(III) MRI contrast agents detailed in Chapters 2 and 3 and the interactions that occur through molecular bonds that are important in molecular magnetic materials (Chapters 3 and 4). The through-space interactions can be described by a dipolar mechanism. The through-bond interactions are a result of the Pauli exclusion principle and the electrostatic interaction between electrons. These interactions depend on the orbital overlap of the orbitals containing the unpaired electrons.

Through-space magnetic interactions: Gadolinium(III) MRI contrast agents

In Gd(III) MRI contrast agents, the electronic paramagnetic moment of the Gd(III) ion interacts with the nuclear spin moment on the hydrogen atoms of water molecules endogenous to the organism under study. The Gd(III) moment is a system with $S = 7/2$ as the Gd(III) ion has seven unpaired electrons, each occupying one of the seven f-orbitals. Since each f-orbital is half occupied the total electron orbital angular

momentum, L, is zero. Thus, unlike other lanthanides, spin-orbit interactions between L and S do not need to be considered for Gd(III). As mentioned above, the spin of the hydrogen nucleus, I, is 1/2.

Gadolinium(III) contrast agents function by catalyzing the relaxation of the nuclear spin moment of the hydrogen nucleus in an external magnetic field. To see how this is the case, it is instructive to consider the pulsed Fourier transform (FT) NMR experiment from a semi-classical, vector representation. Recall from the Zeeman effect section that the spin 1/2 hydrogen nucleus will form a bulk magnetization, $\boldsymbol{M}$, in an applied magnetic field based on Boltzmann population of the two spin states. In a typical FT-NMR experiment, where, for simplicity, we consider a species such as water with all chemically equivalent protons, an RF pulse of the appropriate frequency is applied to the sample at right angles to the applied magnetic field. This tips $\boldsymbol{M}$ away from $\boldsymbol{M_o}$ and the z-axis (defined by $\boldsymbol{H_o}$) and towards the x,y-plane (Figure 1-2). The amount by which $\boldsymbol{M}$ is tipped depends upon the duration and power of the pulse and the frequency of the applied RF field. Since $\boldsymbol{M}$ is essentially a dipole in a magnetic field, it will precess about the z-axis at a frequency known as the Larmor frequency, ω_H. The Larmor frequency is the product of the gyromagnetic ratio, γ_H, of the nucleus under study and the magnitude of the magnetic field, H_o. It is also the resonant frequency of the nucleus and hence must be a component of the applied RF field.

As $\boldsymbol{M}$ precesses, it relaxes back to equilibrium. This is achieved through two pathways, longitudinal relaxation and transverse relaxation. Both processes display first order kinetics and can be characterized by relaxation times T_1 for longitudinal relaxation and T_2 for transverse relaxation. The T_2 route, also known as spin-spin relaxation,

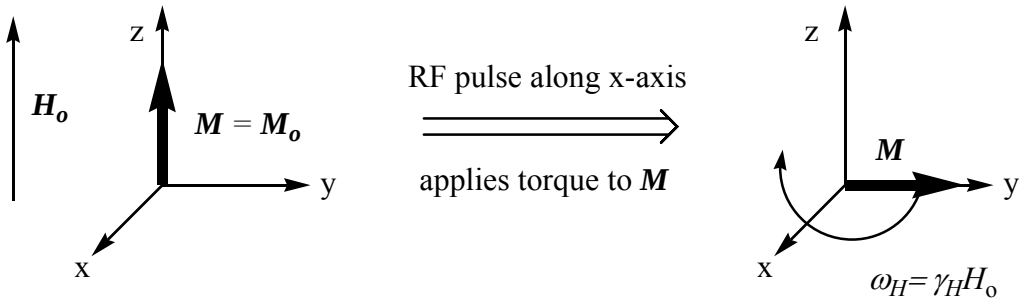

Figure 1-2: Precession of $\boldsymbol{M}$ in the xy-plane results from application of an RF pulse perpendicular to $\boldsymbol{H_o}$.

equilibrates the system in the x,y-plane, while the T_1 process, the spin-lattice relaxation, returns $\boldsymbol{M}$ to the z-axis. It is the latter of these two processes, T_1 relaxation, that is affected by the interaction of the Gd(III) ion with the hydrogen nucleus.

The T_1 MRI experiment weights the response of the water hydrogen nuclei based on their relaxation values. While the application of T_1 weighting in MRI is complicated due to the magnetic field gradients required for spatial resolution, the phenomenon itself can be understood by examining the inversion recovery experiment used to measure T_1. In this experiment, $\boldsymbol{M}$ is tipped 180° so that it points along the negative z-axis. Since there is no x,y-component to $\boldsymbol{M}$, T_2 processes are not in effect. $\boldsymbol{M}$ then relaxes back to the equilibrium position along the positive z-axis. Since the magnetization vector is aligned along the z-axis, it is not possible to detect the relaxation directly. This problem can be circumvented by periodically tipping the $\boldsymbol{M}$ vector into the x,y-plane and measuring the free induction decay (FID). By changing the time delay between the inversion pulse and the detection pulse, and by plotting the delay time versus the magnitude of $\boldsymbol{M}$, an exponential curve can be obtained. Fitting this plot to a mono-exponential function then gives T_1.

In MRI, a spatially resolved unit is known as a voxel. Faster RF pulses can provide higher spatial and temporal resolution and sensitivity, but they give the nuclei less time to relax between scans. Since the mechanisms that couple the nuclear spins to the lattice are inefficient, the nuclear relaxation times are quite long, on the order of seconds. This is a boon to NMR spectroscopy since it gives narrow linewidths due to the uncertainty principle, but it severely limits the sensitivity of an MR image. Reducing T_1 improves sensitivity for the simple reason that the nuclear spins will reach equilibrium

more quickly and can therefore be probed with more scans per unit time. The utility of Gd(III) contrast agents as relaxation catalysts then becomes apparent.

Since the Gd(III) ion does not bond directly with the hydrogen atom on the water molecule, and since the f-orbitals display poor covalency, the interaction between the Gd(III) paramagnetic moment and the nuclear hydrogen spin moment occurs predominantly via a through-space dipole-dipole interaction. The electronic moment of the Gd(III) center is constantly reorienting itself due to inherent electronic relaxation and the tumbling of the ion in solution. This reorientation generates a broad band of frequencies whose distribution starts at zero and tapers off at τ_c^{-1}, where τ_c is the correlation time of the fluctuations. If ω_H is within this range then it couples with the paramagnetic center through space and is effectively relaxed. The distribution of frequencies is summarized in the spectral density function $J(\omega_H, \tau_c)$:

$$J(\omega_H, \tau_c) \propto \frac{\tau_c}{1+\omega_H^2 \tau_c^2} \tag{2}$$

This function is Lorentzian in shape and simple differentiation shows that $J(\omega_H, \tau_c)$ is maximal when $\omega_H = 1/\tau_c$.

The relaxation enhancement of the hydrogen nuclei induced by the Gd(III) ion can be factored into inner-sphere and outer-sphere components. The inner-sphere portion deals with water atoms bound directly to the gadolinium(III) center through a Gd-O bond while the outer-sphere component treats the Gd(III) complex as a hard sphere. The inner-sphere contribution to the T_1 of the hydrogen nucleus can be written as:

$$\left(\frac{1}{T_1}\right)_{i.s.} = \frac{qP_m}{T_{1m} + \tau_m} \tag{3}$$

where P_m is the mole fraction of the contrast agent in the solution, q is the number of inner-sphere water molecules, τ_m is the residency lifetime of the water molecules and i.s. denotes the inner-sphere contribution. It is convenient to define a concentration independent quantity known as the relaxivity, r_1, of a contrast agent. This quantity has the units of $mM^{-1}sec^{-1}$ and is equal to $(1/T_1)$/(contrast agent concentration).

Formally, T_{1m} contains the through-space and through-bond coupling contributions to the relaxivity due to the coordinated inner-sphere water molecules. However, as mentioned above, the through-bond contribution is negligible and T_{1m} closely approximates the dipole-dipole contribution, T_1^{DD}, given below:

$$\frac{1}{T_1^{DD}} = \frac{2}{15}\frac{\gamma_H^2 g^2 \mu_B^2 S(S+1)}{r^6}\left[\frac{3\tau_{c1}}{\left(1+\omega_H^2\tau_{c1}^2\right)} + \frac{7\tau_{c2}}{\left(1+\omega_s^2\tau_{c2}^2\right)}\right] \qquad (4)$$

$$\text{where:} \quad \frac{1}{\tau_{ci}} = \frac{1}{T_{ie}} + \frac{1}{\tau_m} + \frac{1}{\tau_R} \quad i = 1,2 \qquad (5)$$

This is one of the Solomon-Bloembergen-Morgan (SBM) equations. Perusal of Equations 4 and 5 shows how T_1^{DD} depends on the various dynamic processes occurring at the molecular level. The term in front of the brackets represents the maximum magnitude of the dipole-dipole interaction and includes the magnitude of the two moments involved and their distance separation, r. The two terms within the brackets are the spectral density functions for the nuclear spin (the first term) and the electron spin (the second term). The correlation times are comprised of three components, the electronic relaxation time, T_{ie}, the rotational correlation time of the molecule, τ_R, and τ_m. The two characteristic electronic relaxation times, the longitudinal time, T_{1e}, and the transverse time, T_{2e}, are analogous to the nuclear relaxation times discussed above. If any

of these three factors is much faster than the others, it will determine the relaxation enhancement. Recall that the spectral density function is maximal when $\tau_c = 1/\omega_H$ (Equation 2). Thus, efficient water proton relaxation results when the factors influencing τ_c are balanced. The contributions of the various factors to the correlation times are discussed in more detail in the Introduction section of Chapter 3.

Through-bond magnetic interactions: Molecular magnetic materials

Unpaired electrons on different paramagnetic centers may interact with each other through bonds via electrostatics in accordance with the Pauli exclusion principle. This type of interaction is known as an exchange interaction or exchange coupling and dominates the much smaller through-space dipolar interaction by orders of magnitude on the short (interatomic) distance scale. Direct exchange refers to the interaction that occurs between two paramagnetic atoms bound directly to each other. The more commonly observed exchange coupling involves the mediation of the interaction of the unpaired electron spin densities through a diamagnetic bridging ligand or atoms. This type of exchange interaction is known as superexchange. Since superexchange coupling is the focus of Chapters 3 and 4, it will be described using a Cu(II) example and referred to simply as exchange coupling.

The bimetallic copper(II) compound $[Cu_2(tmen)_2(OH)_2](ClO_4)_2$ (tmen = N,N, N',N'-tetramethyethylenediamine) (Figure 1-3) displays exchange coupling between the two paramagnetic spin 1/2 copper centers via the hydroxy bridges. In this compound each copper ion has one unpaired electron in a $d_{x^2-y^2}$ orbital. The spins on each copper center interact with each other through the p-orbitals on the oxygen atoms of the hydroxy

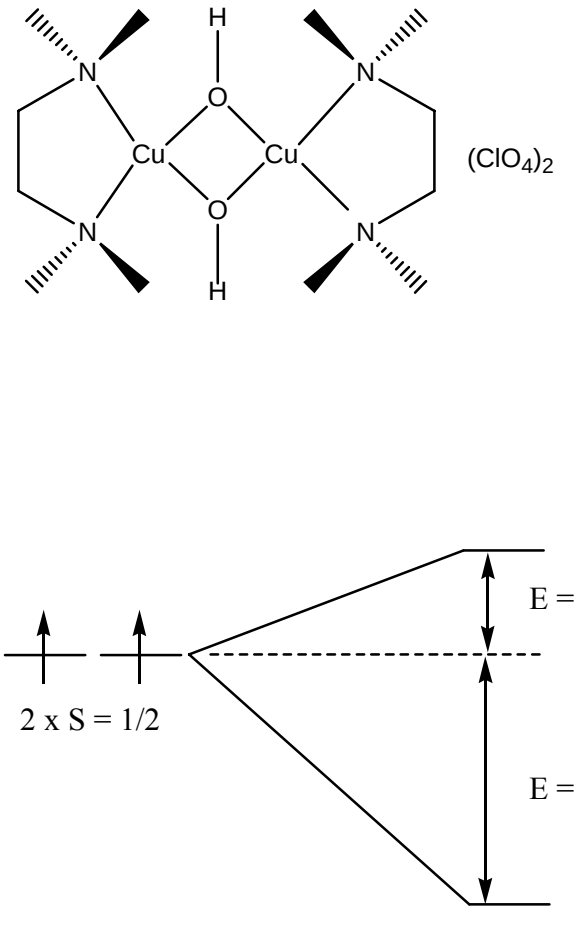

Figure 1-3: The structure of $[Cu_2(tmen)_2(OH)_2](ClO_4)_2$ (top). Each Cu(II) atom adopts a square planar geometry. The splitting of the spin states due to antiferromagnetic exchange coupling (bottom). The energy difference between the states is equal to J.

bridge. The Cu-O-Cu angle determines the extent to which the orbitals are involved in the interaction and has an effect on the nature of the coupling.

In the absence of zero-field effects, the exchange interaction can be described by the Heisenberg spin Hamiltonian:

$$\mathcal{H} = -\mathcal{J}(\mathbf{S_1} \bullet \mathbf{S_2}) \tag{6}$$

where $\mathbf{S_1}$ and $\mathbf{S_2}$ are the spin vectors of each copper atom respectively and $\mathcal{J}$ describes the magnitude of the exchange coupling. This Hamiltonian has the same general form as those used for spin-orbit coupling and hyperfine interactions. In the present copper dimer case the eigenvectors of the Hamiltonian give rise to an $S = 0$ state and an $S = 1$ state where S is now the total spin of the dimer system. It is important to remember that this coupling exists in the absence of any applied fields and describes the spin states of the entire dimer.

The general eigenvalues of the two-spin Heisenberg Hamiltonian are given by:

$$E_S = -1/2\mathcal{J}[S(S+1) - S_1(S_1+1) - S_2(S_2+1)] \tag{7}$$

Thus the copper dimer case generates $E_{S=0} = 3/4\ \mathcal{J}$ and $E_{S=1} = -1/4\ \mathcal{J}$ with a total energy difference of $\mathcal{J}$. If $\mathcal{J}$ is positive then the $S = 1$ state will be lower in energy, while a negative value results in $S = 0$ being more stable. As the $S = 1$ state corresponds to a parallel alignment of spins, a positive $\mathcal{J}$ value indicates ferromagnetic coupling. With $S = 0$ the spins are aligned anti-parallel and thus antiferromagnetic coupling will have a negative $\mathcal{J}$ value. The magnitude of the exchange coupling reflects the strength of the interaction and hence the degree of orbital overlap along the superexchange pathway. Better overlap typically results in a larger magnitude coupling (Chapter 3).

The value of J can be determined by fitting the experimental magnetic susceptibility as a function of temperature to a Boltzmann population distribution of the spin states resulting from the Heisenberg Hamiltonian. This can be readily performed for the copper system and gives a J value of -180 cm^{-1}. The negative value indicates antiferromagnetic coupling.

Examination of the orbital pathway between the unpaired electrons provides an initial hypothesis about the nature of the exchange coupling and the sign of J. If the orbitals are orthogonal to each other then the interaction will be ferromagnetic; this is the case for the Ru(III)-Ni(II) compound in Chapter 4. The unpaired electron in the Ru(III) ion resides in a d-orbital that interacts with the π-orbitals on the cyanide bridge, whereas the two unpaired electrons in the Ni(II) ion are in d-orbitals that interact with cyanide σ-orbitals. The σ- and π-orbitals are orthogonal so the interaction is ferromagnetic. Ferromagnetic coupling is the exception rather than the rule; most exchange interactions are antiferromagnetic like the copper dimer example above. In these cases the orbital pathway, which can depend strongly on bond angles, does not contain an orthogonality so the electrons must couple antiferromagnetically.

Although examination of the orbital pathways can give insight into the expected coupling, the nature of the coupling is best determined by measurement of the saturation magnetization of the compound. In this measurement the temperature is low, thus the lowest energy spin states will be the only states thermally occupied. The applied magnetic field is high in these measurements as well, so the Zeeman splitting of the lowest energy total spin states will be large. Thus, the saturation magnetization will typically reflect the lowest energy spin level and provide a direct measure of the nature of

the coupling. In some instances there may be several levels close enough in energy to complicate interpretation of the saturation magnetization. This is the case in Chapter 4 where the zero field splitting of the Ru(III) ion gives a saturation magnetization that deviates from the spin-only value.

The discussion of exchange coupling thus far has focused on the isotropic interaction between two ions. This is a short-range exchange interaction and gives rises to paramagnetic behavior that reflects the magnetism resulting from the interaction of a few spin centers. In bulk ferro-, ferri- and antiferromagnetic non-conducting systems the interactions are similar to the case described above but occur throughout the material and can contain anisotropic components. Overall, these interactions are difficult to describe but give rise to the long-range magnetic ordering seen in these materials. The magnetic exchange interaction also gives rise to the coupling and splitting of peaks seen in the NMR spectra of diamagnetic species. In this case the interacting spins are the nuclear spins, but the interaction is mediated by the electrons as it is in the paramagnetic copper case above.

Scope of the Thesis

This chapter provides an introduction into the magnetic effects that are discussed in the remainder of the dissertation. After an overview of the properties of matter that generate magnetism, the chapter details the interaction between quantum angular momentum and magnetic fields embodied in the Zeeman effect. This is followed by an examination of the different types of magnetism beginning with diamagnetism and paramagnetism. The chapter then proceeds to discuss the long-range magnetic order

observed in ferromagnetic, antiferromagnetic and superparamagnetic systems. The through-space effect a paramagnetic ion has on paramagnetic nuclear spins is then discussed. This is related to the specific example of Gd(III) ions interacting with water molecule hydrogen nuclei and provides the fundamentals for Chapters 2 and 3. The through-bond magnetic exchange interaction is then introduced and described for molecular systems using the canonical copper(II) dimer system. The exchange interaction is discussed further in Chapters 3 and 4.

Chapter 2 focuses on modulation of q to produce a biochemically activatable MRI contrast agent. This research is based on previous work involving the compounds known as EGad and EGadMe (Figure 1-4). In the EGad system, the relaxation modulation is provided by opening up a coordination site at the Gd(III) metal center through enzymatic hydrolysis of a water blocking moiety, thus converting the agent from a weak relaxivity r_{weak} to a stronger relaxivity, r_{strong}, through an increase in q. The β-glucuronidase sensitive agent discussed in Chapter 2 explores the utility of endogenous anions, particularly carbonate, in modulating relaxivity via chelation to seven-coordinate Gd(III) complexes. The enzymatic hydrolysis of β-glucuronic acid from the contrast agent converts the agent to an eight-coordinate Gd(III) chelate. The relaxivity of the agent before and after enzyme catalyzed hydrolysis is examined in a variety of buffers and as a function of bicarbonate concentration. The enzyme kinetics are then studied to assess the effect the self-immolative linker has on the biochemistry of the agent.

Chapter 3 examines the possibility of relaxivity modulation in MRI contrast agents via changing T_e. This work makes use of both the through-space and through-bond magnetic interactions discussed in Chapter 1. The through-space effect occurs

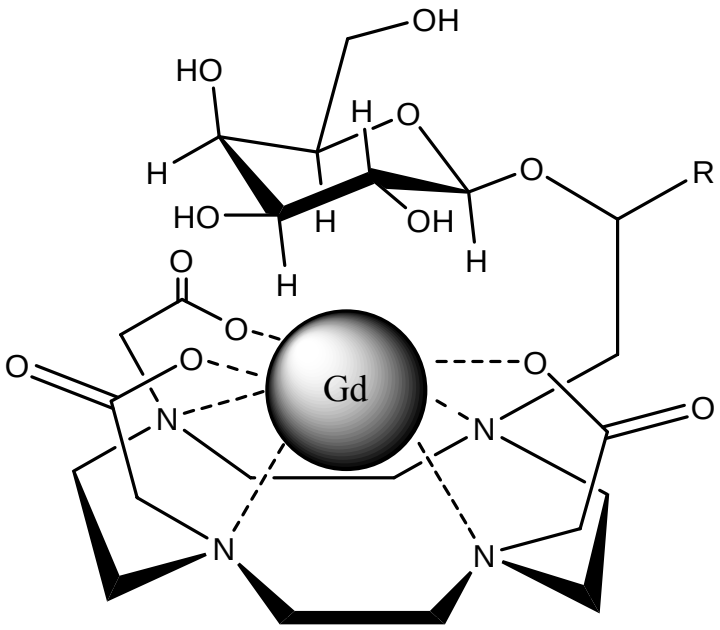

Figure 1-4: The structure of the MRI contrast agents known as EGad (R = H) and EGadMe (R = methyl). The structure is drawn to indicate the hypothesized water blocking ability of the sugar group.

between the hydrogen nuclei and Gd(III) ions while the through-bond interactions are anticipated to modulate T_e of the Gd(III) center through the oxidation and reduction of an adjacent ruthenium ion. The chapter begins with a proposed Ru-Gd dyad based on a similar known geometry for Cu-Gd dyads. Subsequent work showed that Gd(III) was not chelated effectively by the ligand set. Furthermore, evidence was obtained for the dimerization of the Ru(III) precursor. The chapter then details research using a ligand designed to provide better chelation of Gd(III). It was found that this ligand set is susceptible to hydrolysis. Thus the chapter concludes with the steps taken towards a ligand set that addresses the shortcomings of the preceding two systems.

The dimerization observed in Chapter 3 formed the basis for the Ru(III)-Ni(II) one dimensional coordination polymer discussed in Chapter 4. This system uses the linear cyanide ligand to effectively bridge the two paramagnetic centers. The chapter begins with a discussion of the techniques used to characterize low dimensional magnetic materials, building on the background presented in Chapter 1. The structural aspects of the Ru(III) precursors and the coordination polymer are then discussed. This is followed by magnetic studies on the system. The results of the studies indicate that the Ru(III) and Ni(II) centers are ferromagnetically coupled but do not display long-range magnetic interactions above 3 K.

References

Ashcroft, N.W., Mermin, N.D.: *Solid State Physics.* Saunders College; Harcourt Brace, Orlando 1976.

Banci, L., Bertini, I., Luchinat, C.: *Nuclear and electron relaxation: The magnetic nucleus-unpaired electron coupling in solution.* VCH, Weinheim; New York 1991.

Caravan, P., Ellison, J.J., McMurry, T.J., Lauffer, R.B. (1999) Gadolinium(III) chelates as MRI contrast agents: Structure, dynamics, and application. *Chemical Reviews,* **99**: 2293-2352.

Chandramouli, G.V.R., Kundu, T.K., Manoharan, P.T. (2003) Magneto-structural correlation in di-μ-oxo bridged dicopper complexes. Predictability of isotropic exchange-coupling constant from structure. *Australian Journal of Chemistry,* **56**: 1239-1248.

Drago, R. S.: *Physical Methods for Chemists 2ed.* Saunders College; Harcourt Brace, Orlando 1992.

Itoh, K., Kinoshita, M.: *Molecular magnetism: New magnetic materials.* Kodansha; Gordon and Breach, Tokyo; Amsterdam 2000.

Kahn, O.: *Molecular Magnetism.* Wiley-VCH, New York 1993.

Kittel, C.: *Introduction to Solid State Physics 7ed.* Wiley, New York 1995.

Louie, A.Y., Huber, M.M., Ahrens, E.T., Rothbacher, U., Moats, R., Jacobs, R.E., Fraser, S.E., Meade, T.J. (2000) In vivo visualization of gene expression using magnetic resonance imaging. *Nature Biotechnology,* **18**: 321-325.

Merbach, A.E., Toth, E.: *The chemistry of contrast agents in medical magnetic resonance imaging.* John Wiley and Sons, West Sussex; New York 2001.

Orchard, A.F.: *Magnetochemistry.* Oxford University, Oxford; New York 2003.